

1 **Measurement Report: Urban Ammonia and Amines in Houston, Texas**

2
3 Lee Tiszenkel¹, James Flynn², Shan-Hu Lee^{1*}

4
5 ¹ Department of Atmospheric and Earth Sciences, University of Alabama at Huntsville;
6 Huntsville, Alabama, USA

7 ² Department of Earth and Atmospheric Sciences, University of Houston; Houston, Texas,
8 USA

9
10 Corresponding author (shanhu.lee@uah.edu)

11

12 **Abstract.** Ammonia and amines play critical roles in secondary aerosol formation, especially in
13 urban environments. However, fast measurements of ammonia and amines in the atmosphere are
14 very scarce. We measured ammonia and amines with a chemical ionization mass spectrometer
15 (CIMS) at the urban center in Houston, Texas, the fourth most populated urban site in the United
16 States, during October 2022. Ammonia concentrations were on average 4 parts per billion in
17 volume (ppbv), while the concentration of an individual amine ranged from several parts per
18 trillion in volume (pptv) to hundreds of pptv. These reduced nitrogen compounds were more
19 abundant during the weekdays than on weekends and correlated with measured CO concentrations,
20 implying they were mostly emitted from pollutant sources. Both ammonia and amines showed a
21 distinct diurnal cycle, with higher concentrations in the warmer afternoon, indicating dominant
22 gas-to-particle conversion processes taking place with the changing ambient temperatures. Studies
23 have shown that dimethylamine is critical for urban new particle formation (NPF), but currently,
24 there are no amine emission inventories in global climate models (as opposed to ammonia). Our
25 observations show that amines in general positively correlated with ammonia, indicating that it is
26 reasonable for global models to use scaled-down ammonia concentrations (e.g., 0.1 %) as a proxy
27 of urban dimethylamine concentrations to simulate urban NPF processes.

28 **1. Introduction**

29 Atmospheric ammonia and amines are ubiquitous in the atmosphere, and they have been found
30 in the gas phase, aerosol, clouds, and fog droplets [*Ge et al.*, 2011a; b]. Ammonia and amines are
31 emitted from various natural and anthropogenic sources, such as agricultural activity, animal
32 husbandry, vegetation, soil, waste processing, automobile traffic, power plants, and biomass
33 burning [*Ge et al.*, 2011a]. Ammonia and amines often share the same emission sources. In general,
34 ambient concentrations of ammonia are at the parts per billion in volume (ppbv) range, and amines
35 are approximately two to three orders of magnitude lower than ammonia concentrations. Ambient
36 concentrations of ammonia and amines vary rapidly due to emission, gas-to-particle conversion,
37 and wet deposition processes [*You et al.*, 2014; *Yu and Lee*, 2012].

38 Laboratory studies have shown that ammonia and amines play key roles in new particle
39 formation (NPF) as they can stabilize sulfuric acid clusters [*Almeida et al.*, 2013; *Glasoe et al.*,
40 2015; *Jen et al.*, 2016; *Lehtipalo et al.*, 2018; *M Xiao et al.*, 2021; *Yu et al.*, 2012]. In particular,
41 dimethylamine can have a profound effect on atmospheric processes even at the pptv level
42 [*Almeida et al.*, 2013; *Glasoe et al.*, 2015]. Field observations show that ammonia and amines are
43 associated with NPF events in Chinese megacities [*R. Cai et al.*, 2021; *Runlong Cai et al.*, 2023;
44 *Yan et al.*, 2021; *Yao et al.*, 2016], urban areas in the United States [*Jen et al.*, 2016; *Smith et al.*,
45 2010], European cities [*J. Brean et al.*, 2020], a high altitude site [*Bianchi et al.*, 2016], and the
46 Arctic and Antarctic [*Beck et al.*, 2021; *James Brean et al.*, 2021; *Jokinen et al.*; *Köllner et al.*,
47 2017]. However, global models cannot simulate urban NPF processes currently because of the lack
48 of amine emission inventories in models.

49 Ammonia and amines also contribute to secondary organic aerosol (SOA) formation by
50 condensation of oxidation products formed by reactions with ozone, OH, or NO₃ radicals and

51 produce light-absorbing particles [*Mark E. Erupe et al.*, 2010; *Malloy et al.*, 2009; *C. J. Nielsen*,
52 2016; *Claus J. Nielsen et al.*, 2012; *Qiu and Zhang*, 2013; *Silva et al.*, 2008]. As a result, reducing
53 ammonia emissions has been identified as a cost-effective way to mitigate ambient fine particle
54 concentrations [*Gu et al.*, 2021].

55 Fast-response measurements of ammonia and amines at atmospheric concentrations are very
56 challenging [*Lee*, 2022], although such measurements are necessary because these reduced
57 nitrogen compounds have relatively short atmospheric lifetimes [*Claus J. Nielsen et al.*, 2012].
58 Previously, [*Schwab et al.*, 2007] made an intercomparison of six different ammonia detection
59 methods in the laboratory and found a large variance in the measured concentrations and vastly
60 different response times (over several hours) within different instruments. Difficulties in the
61 detection of base compounds also arise because these “sticky” compounds can rapidly adsorb and
62 desorb on/from the surfaces of sampling inlets to cause background signals that vary depending
63 on ambient concentrations, air humidity, and other atmospheric conditions. Thus frequent, in situ
64 measurements of instrument background signals using proper zero gases are required, especially
65 for field observations with rapidly changing ambient concentrations of base compounds.

66 Chemical ionization mass spectrometers (CIMS) using ion reagents such as protonated ethanol,
67 acetone, and water ions can detect ammonia and amines in the atmosphere with fast response
68 [*Benson et al.*, 2010; *Hanson et al.*, 2011; *Jen et al.*, 2016; *Nowak et al.*, 2006; *Nowak et al.*, 2010;
69 *Yu and Lee*, 2012]. As summarized in Table 1, CIMS technique has been used for the detection
70 of ambient ammonia and amines at a polluted site in Ohio [*You et al.*, 2014; *Yu and Lee*, 2012], a
71 rural Alabama forest [*You et al.*, 2014], and polluted urban sites in China [*G Wang et al.*, 2016; *M*
72 *Wang et al.*, 2020a; *Zheng et al.*, 2015; *Zhu et al.*, 2022]. As shown in Table 1, there are even
73 fewer studies that simultaneously measured ammonia and amines. The CIMS using ethanol reagent
74 can measure amines at or below single-digit pptv concentrations with a time response of 1 minute
75 and measure simultaneously amines and ammonia [*Benson et al.*, 2010; *M. E. Erupe et al.*, 2011;
76 *You et al.*, 2014; *Yu and Lee*, 2012]. The CIMS using protonated water ions (i.e., proton-transfer
77 chemical ionization mass spectrometer, PTR-CIMS) can measure mono- and di-amines [*Hanson*
78 *et al.*, 2011; *Jen et al.*, 2016]. Using a high-resolution time-of-flight (HR-TOF) detector coupled
79 to CIMS (HR-TOF CIMS) (with ethanol reagent), [*Yao et al.*, 2016] measured various amines and
80 amides in Shanghai. However, isomers of amines were still not resolved in the detection; for
81 example, the measured C2-amines still contained dimethylamine and ethylamine. Thus, a major
82 disadvantage of a mass spectrometer (regardless of mass resolution) is the inability to
83 resolve/identify isomers. To resolve isomers, tandem MS/MS analysis or an additional
84 independent separation method (such as chromatography) coupled to the mass spectrometer is
85 necessary.

86 In situ measurements of ammonia have been made in various atmospheric environments also
87 with optical techniques such as open-path absorption [*Miller et al.*, 2014], closed-path absorption
88 [*Ellis et al.*, 2010; *Griffith and Galle*, 2000; *Leen et al.*, 2013; *McManus et al.*, 2010; *Pollack et*
89 *al.*, 2019], cavity ring-down spectroscopy [*Martin et al.*, 2016], and photoacoustic spectroscopy

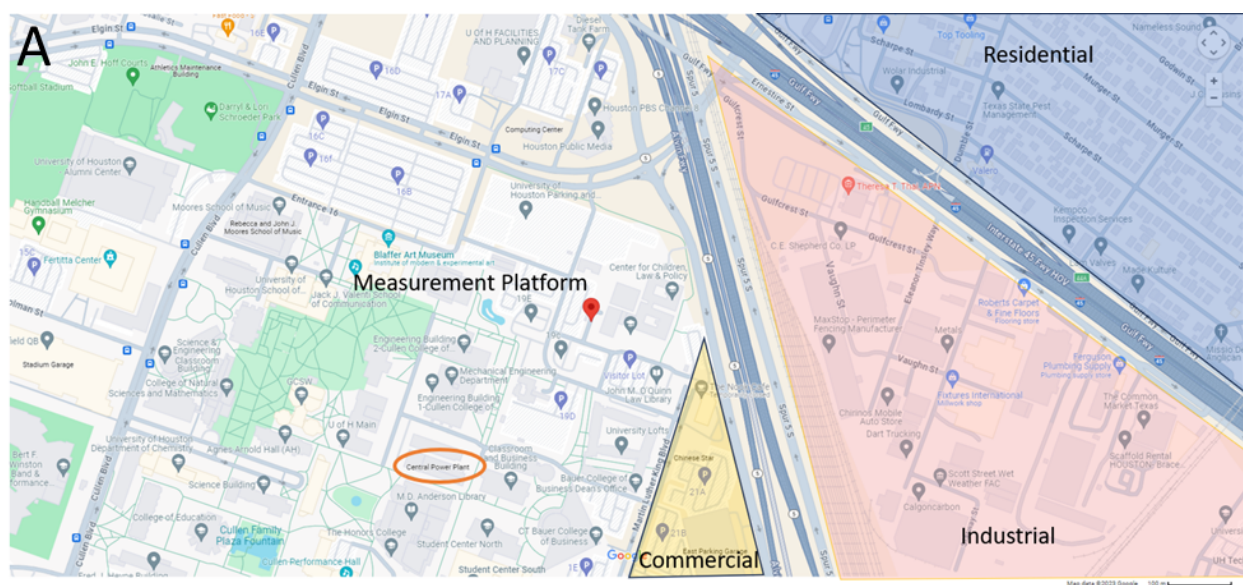
90 [Pushkarsky *et al.*, 2002]. These fast-response optical techniques were used for flux and aircraft
91 measurements of ammonia.

92 We measured ammonia and C1-C6 amines with an ethanol CIMS in October 2022 at the urban
93 center in Houston, Texas. Houston is the fourth most populated urban center in the U.S. and
94 contains a diverse range of pollutant emissions from urban activity, traffic, ship channels, oil
95 production, marine air masses, and agricultural activity. The primary goal of these measurements
96 is to quantify ammonia and C1-C6 amines in an urban setting and identify the atmospheric
97 conditions that affect their abundance. The study is amongst very few observations of ammonia
98 and amines at highly polluted urban sites in the U.S. We also compare observations in Houston
99 with previous measurements taken with the same instrument in Kent, Ohio (less polluted) [You *et*
100 *al.*, 2014] and establish a quantitative relationship between ammonia and dimethylamine in a
101 different range of polluted conditions. This relationship will allow global models to simulate urban
102 NPF processes using the existing ammonia emission inventories.

103

104 2. Methods

105



106

107

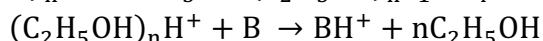
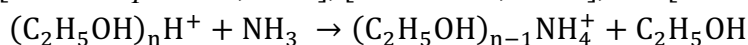
108 **Figure 1.** Location of the measurement platform, indicated by a red pin in the center of the map.
109 Nearby commercial, industrial, and residential areas are labeled by yellow, red, and blue shaded
110 sections, respectively. The nearby University of Houston power plant is circled in orange to the
111 southwest of the measurement platform. The map of the greater Houston urban area, as well as
112 the satellite view of the nearby vicinity of the measurement site, are shown in Figure S1.

113

114 The field observation took place in Houston continuously from the 8th to the 27th of October in
115 2022. Measurements were made at a stationary platform located on the campus of the University
116 of Houston (29.72° N, 95.34° W) ~2.5 km from central downtown Houston. Maps of the
117 measurement site (Figures 1 and S1). The measurement platform was located ~5 m from an active

118 parking lot, ~200 m from a low-traffic road, ~300 m from a high-traffic thoroughfare, and ~500 m
119 from an interstate highway. The immediate vicinity of the site was the University of Houston
120 campus, containing classroom buildings, dormitories, facilities services, and dining halls. Nearby
121 to the southeast of the site were several restaurants as well as an industrial park containing sites of
122 chemical supply companies, construction, machining services, and automobile shops. The site was
123 surrounded by residential areas to the south, northeast, and west. The city center and highest
124 population densities were to the northeast of the measurement site.

125
126 The ethanol CIMS instrument used has been described in detail previously [*Benson et al.*,
127 2010; *You et al.*, 2014; *Yu and Lee*, 2012]. The CIMS draws 10 standard liter per minute (slpm)
128 of sample air into a low-pressure ion-molecule region (about 2,000 Pa) where the flow mixes with
129 a pure nitrogen flow with a 2 slpm through a stainless-steel vessel of 200-proof ethanol, followed
130 by a ^{210}Po radiation source. Ammonia and amines were detected with the following ion-molecule
131 reactions based on [*M. E. Erupe et al.*, 2011], [*Yu and Lee*, 2012], and [*Nowak et al.*, 2006]:



134 Here, “B” refers to amines, and “n” is the number of reagent ions measured by the CIMS (n=1-3).
135 The $(C_2H_5OH)_2H^+$ (m/z = 93) peak was the highest among the three reagent ions (m/z = 47, 93,
136 and 140). As shown in Figure S2, the production ions of amines were protonated ions: C1-amine
137 (m/z = 32), C2 (m/z = 46), C3 (m/z = 60), C4 (m/z = 74), C5 (m/z = 88), and C6 (m/z = 102).
138 Ammonia product ions were NH_4^+ (m/z = 18, higher peak) and $(C_2H_5OH)NH_4^+$ (m/z = 64, lower
139 peak); these two ions were strongly correlated to each other during the ammonia calibration and
140 ambient measurements, indicating they represent ammonia signals.

141 To obtain a background signal, the CIMS is operated with 10 minutes of sampling followed
142 by 10 minutes of background measurements. Figure S2 shows the main reagent and base
143 compound product ions during the switching between ambient and background measurements.
144 Background measurements were taken by switching a 3-way valve to supply the inlet with a flow
145 of zero air through a silicon phosphate medium (Pan Tech, Texas) to scrub ammonia and amines.
146 The reagent signal was taken as the sum of three ethanol reagent ions. Reagent ion signals were
147 typically around 400 kHz with less than 10 % difference between ambient and background
148 measurement modes. Ammonia and amine concentrations were calculated by the difference
149 between the ambient and background signals normalized to 1,000,000 Hz of reagent ion signal
150 multiplied by a calibration factor. Calibration of the instrument was carried out with diluted
151 ammonia in nitrogen and permeation tubes of methylamine, dimethylamine, trimethylamine,
152 diethylamine, and diisopropylamine (Kin-tek, USA). Due to the difficulty of obtaining a
153 calibration standard, C5 amines were assumed to have the same sensitivity as C6 amines. The
154 calibration factors for each compound and detection limits were found to be similar to the results
155 from the calibration of the instrument by [*You et al.*, 2014] (Table S1), over a period of nearly 10
156 years, demonstrating an excellent reproducibility in the instrument performance. The time
157 response of the CIMS instrument to ammonia and amines is defined as where the signal stabilizes

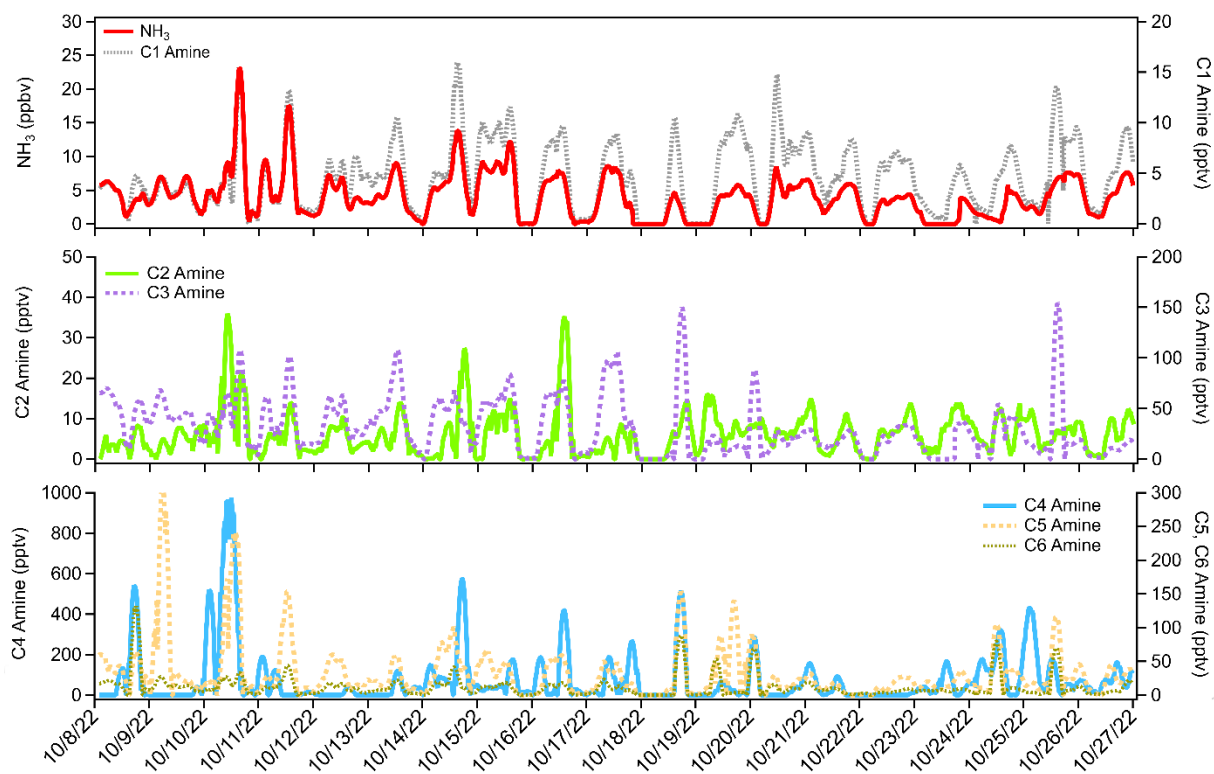
158 at its “double e-folded” concentration of $1/e^2$ during the calibration. Average response times for
159 ammonia and amines were smaller than 1 minute. For each 10-minute cycle of background and
160 measurement, the first two minutes of each background/measurement cycle were excluded from
161 the data analysis to allow the instrument to reach a steady concentration.

162 The uncertainty in the CIMS included error in the permeation sources, which ranged from 2%
163 to 5% depending on the compound. The permeation sources were diluted in two stages using flow
164 controllers that each had uncertainties of 1.5%. Total error in the calibration of the CIMS was
165 6.7%. Overall uncertainty in the CIMS was 30%, accounting for calibration error, variability of
166 ion signals, and inlet losses.

167 Meteorological data was measured concurrently on the platform by a Vaisala HMP-45c for
168 temperature and relative humidity, and a RM Young 05305 wind speed and direction sensor.
169 Additionally, CO and NO_x (NO+NO₂) were measured with Thermo 48c and Thermo 42c-TL,
170 respectively. These measurements were provided by the University of Houston. The uncertainty
171 in trace gas (CO and NO_x) measurements arises from instrumental uncertainty in the Thermo 48c
172 CO analyzer and Thermo 42c-TL NO_x analyzer. Zero correction was performed on this instrument
173 daily by switching to a flow of zero air. The typical uncertainty of each of these instruments was
174 5%.

175
176
177
178

3. Results and Discussion

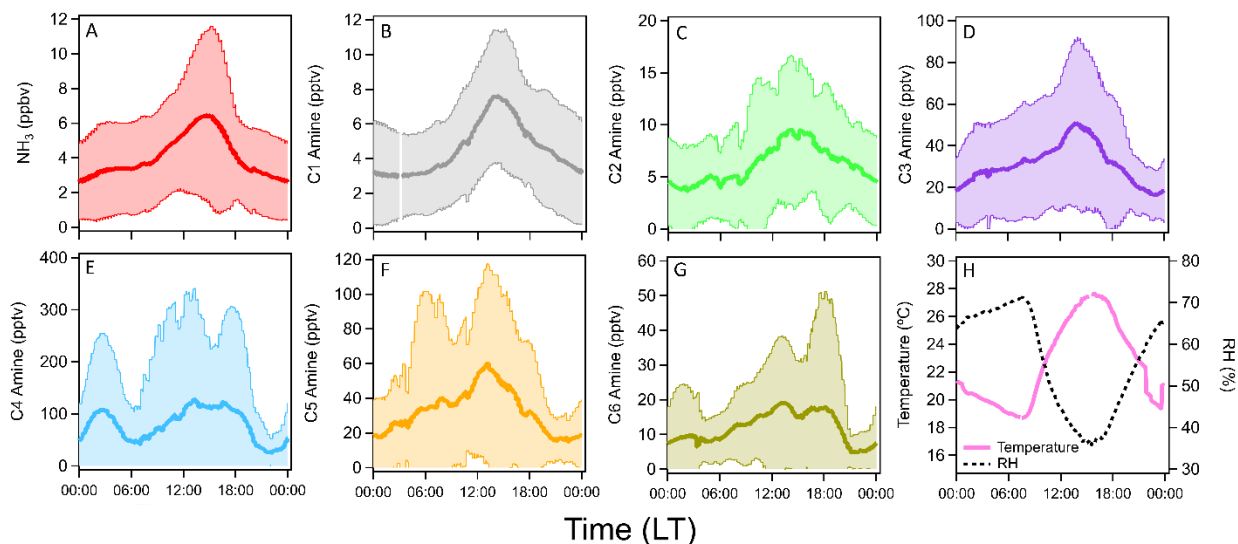


179

180 **Figure 2.** Time series of ammonia and C1-C6 amines observed at the urban center in Houston,
181 Texas, in October 2022.

182 The time series of ammonia and amines during the ambient measurement period is shown in
183 Figure 2. The average ammonia concentration during the measurement campaign was 4 ppbv with
184 several short-term spikes above 10 ppbv and one occasion when the concentration exceeded 20
185 ppbv. Concentrations of C1 amine averaged 4 pptv with several spikes up to 15 pptv. Average C2
186 amine concentrations were 6 pptv with frequent but brief periods of concentrations more than 10
187 pptv. Average C3 amine concentrations were 31 pptv with brief increases in concentration above
188 100 pptv. C4 amine was the most abundant amine observed during the measurement period with
189 an average concentration of 79 pptv with spikes in concentration into the hundreds of pptv.
190 Average C5 and C6 amine concentrations were 33 and 12 pptv, respectively. These concentrations
191 in Houston were generally consistent with concentrations measured in other urban sites (Table 1).
192 Previous CIMS ammonia measurements from aircraft flights above Houston observed similar
193 baseline concentrations of ammonia (0.2-3 ppbv) with brief spikes in concentration (up to 80 ppbv)
194 associated with agricultural or industrial activity [Nowak *et al.*, 2010]. Additionally, ammonia
195 concentrations of similar magnitude to the high spikes in concentration observed in this study have
196 been reported in Shanghai [S Xiao *et al.*, 2015] as well as an urban site in Romania [Petrus *et al.*,
197 2022], with high ammonia concentrations corresponding to high temperatures and high traffic
198 activity. Long-term measurements taken in Nanjing with a cavity ring-down spectrometer also
199 showed an average ammonia concentration of 12 ppbv [Liu *et al.*, 2024]. Measurements of amines
200 in Atlanta, Georgia showed <1 to 3 pptv concentrations of C1 and C2 amines, and C3 and C6
201 amines up to 15-25 pptv [Hanson *et al.*, 2011]. Yao *et al.* [Yao *et al.*, 2016] measured amines at
202 the level of pptv or sub-pptv, e.g., C2 amines of 3.9 ± 1.2 pptv, in urban Shanghai during the
203 summer. It is possible that measured concentrations of amines measured here contain some
204 interference from amides formed from oxidation of emitted amines. The CIMS does not have
205 sufficient resolving power to separate trimethylamine (m/z 59.11) from acetamide (m/z 59.07), for
206 example. Therefore, these amine concentrations represent an upper limit of amine concentrations
207 (assuming all of the detected signal is due to the presence of amines). However, [Yao *et al.*, 2016]
208 measured amide concentrations in urban Shanghai in the tens to hundreds of pptv, while C1-C2
209 amine concentrations in Shanghai were similar to Houston observations reported here. Considering
210 the consistency between amine measurements at these two urban locations, it is likely that
211 interference from amides in the CIMS was minimal for C1 and C2 amines. The discrepancies
212 between these two urban areas become more pronounced for C3-C6 amines (Table 1), which
213 makes amide interference a possible explanation for elevated concentrations of C3 amines and
214 above.

215



216

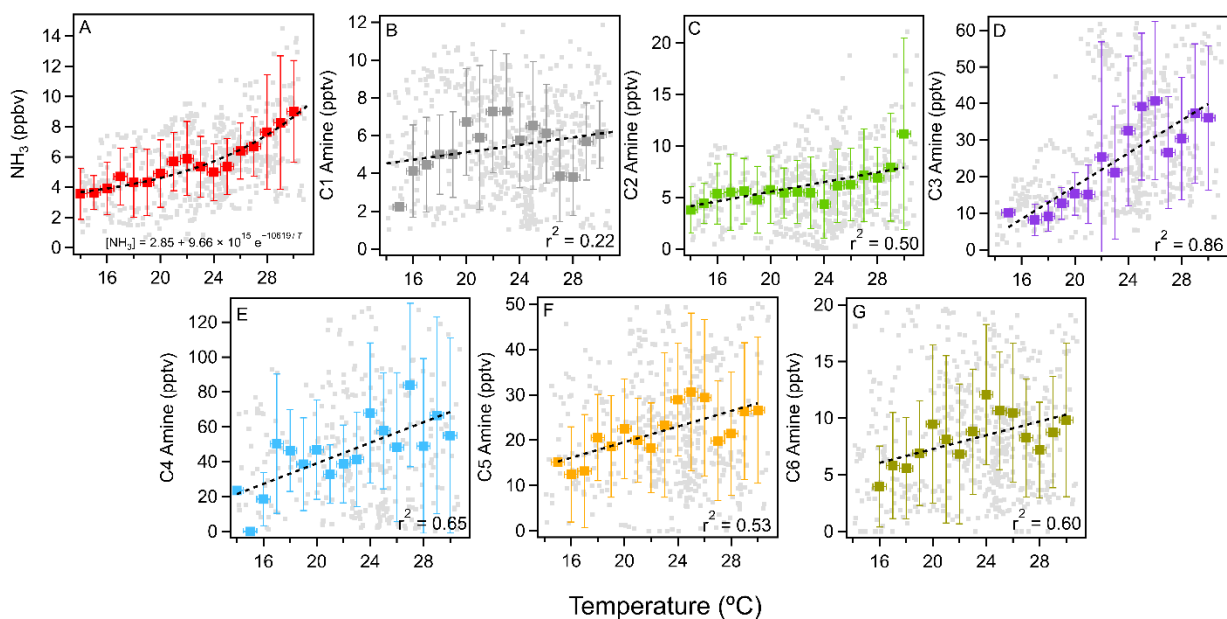
217 **Figure 3.** Averaged diurnal cycles of (a) ammonia, (b-g) C1-C6 amines, (h) temperature, and RH
 218 in Houston, Texas, during the observation period (19 days continuously). Shaded areas indicate 1
 219 standard deviation from the mean values of observation data.

220 Figure 3 shows the averaged diurnal concentrations of ammonia and amines during the
 221 observation period. Ammonia and amines had a diurnal cycle with peak concentrations in the
 222 afternoon with higher ambient temperatures. Generally, ammonia and amines correlated with one
 223 another throughout the measurement campaign, while C1-C3 amines showed the highest
 224 correlation with ammonia. Peak concentrations of all compounds corresponded with the high
 225 temperature of the day at around 3 pm local time. This was especially pronounced for ammonia,
 226 C1 and C3 amines. The relationships between ammonia and amines and temperature are shown in
 227 Figure 4. Ammonia had the strongest correlation with temperature, and the relationship fit an
 228 exponential parameterization, as the following:

$$229 \quad [NH_3] = 2.85 + 9.66 \times 10^{15} e^{-\frac{10619}{T}}$$

230 Amines generally showed linear relationships with temperature, with C3 and C4 amines displaying
 231 the strongest relationships. C3 amines increased by 2.3 pptv per °C ($r^2 = 0.86$) and C4 by 2.9 pptv
 232 per °C ($r^2 = 0.65$). C5 and C6 amines were also moderately correlated with temperature, increasing
 233 by 1.2 pptv per °C and 0.5 pptv per °C, respectively ($r^2 = 0.60$ for both C5 and C6). On the other
 234 hand, the correlation of C1 and C2 amines with temperature were weaker: C1 only increased by
 235 0.1 pptv per °C with almost no correlation ($r^2 = 0.22$), and C2 increased by 0.8 pptv per °C ($r^2 =$
 236 0.50). The temperature dependence of ammonia and amines was previously observed in a rural
 237 forest in Alabama by [You *et al.*, 2014], which attributed this partially to particle-to-gas conversion
 238 of ammonia and amine containing particles at elevated temperatures. The temperature dependence
 239 could also be due to higher emissions at higher temperatures. The temperature dependence of
 240 ammonia and amines has been observed at other urban, suburban and rural locations such as Kent,

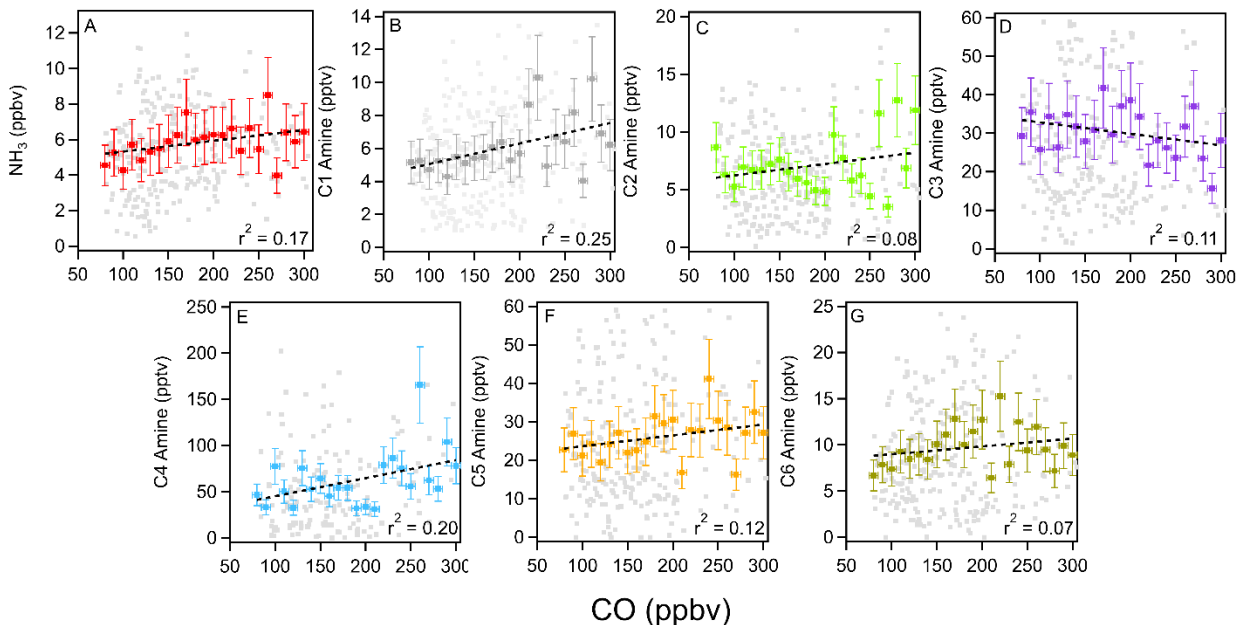
241 Ohio [You et al., 2014], Atlanta [Hanson et al., 2011], Delaware [Freshour et al., 2014], the
 242 Southern Great Plains [Freshour et al., 2014], and rural central Germany [Kürten et al., 2016].
 243



244
 245

246 **Figure 4.** Temperature dependence of (a) ammonia and (b-g) C1-C6 amines measured in Houston.
 247 Vertical bars indicate 1 standard deviation from the mean values of observation data. Binned
 248 temperatures are shown in colored squares, 1-minute averaged data is shown in gray squares.
 249 Horizontal bars indicate bin width. Black dashed lines indicate exponential fit for ammonia and
 250 linear fits for amines.

251 Anthropogenic pollutants such as CO and NO_x and CO can serve as tracers for industrial and
 252 traffic activities. Ammonia and amines in general showed a positive correlation with CO, with the
 253 exception of C3 amines (Figure 5). As ammonia, amines, and CO can be traced to traffic or
 254 industrial emissions, the positive relationship between these compounds implies that these base
 255 compounds were emitted from pollutant sources. Unlike with CO, there was a negative correlation
 256 with NO_x (Figure S3). This lack of a strong correlation between NO_x and ammonia was previously
 257 observed in Nanjing where a strong reduction in NO_x concentration during COVID-19 lockdown
 258 periods was not accompanied by an equivalent reduction in ammonia concentrations [Liu et al.,
 259 2024]. This may indicate some unique emission sources for ammonia and amines that do not co-
 260 emit NO_x.
 261

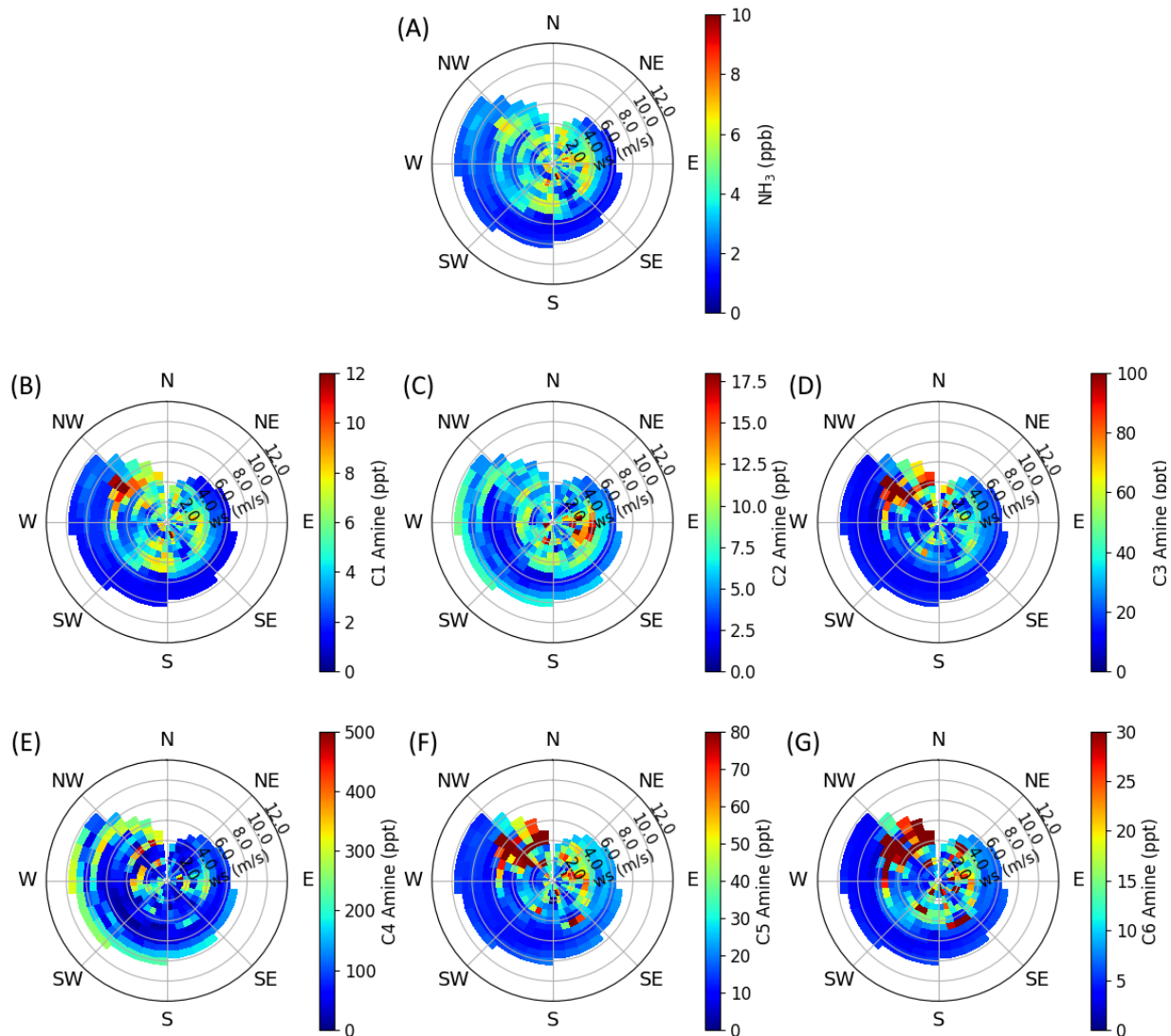


262
 263 **Figure 5.** Correlation between ammonia (a) and C1-C6 amines (b-g) with the collocated CO
 264 concentrations during the measurement campaign. Binned CO concentrations are shown in colored
 265 squares, 5-minute averaged data shown in gray squares. Vertical bars indicate 1 standard deviation
 266 from the mean values of observation data. Horizontal bars indicate bin widths. Black dashed lines
 267 indicate linear fits.

268 Wind speed and direction can help to identify local sources of ammonia and amines near the
 269 measurement site. Figures 6 and S4 show the correlation of ammonia and amines with wind speeds
 270 and direction throughout the observation period. Consistent between all base compounds is the
 271 high concentration coming from the southeast. This is the direction of the interstate highway,
 272 industrial areas, and train yards (Figures 1 and S1). Ammonia and most amines also have a
 273 pronounced source from the northwest – this is the direction of downtown Houston, where
 274 population density is highest. Except for C2 and C4 amines, the observed ammonia and amines in
 275 Houston were higher during periods of low wind speeds. The abundant C2 and C4 at high wind
 276 speeds may suggest that C2 and C4 amines were transported from more distant sources.

277 Figure S5 shows the average diurnal cycle of ammonia and amines on weekdays as opposed
 278 to weekends. Except for C2 and C4 amines, there was a clear decrease in concentrations during
 279 weekends during the afternoon peak. Weekends saw much less traffic and activity on the
 280 University of Houston campus. During this observation period, ambient temperatures were higher
 281 during the weekends, which would increase emissions. Therefore, the differences in weekdays vs.
 282 weekends indicate that amines and ammonia were indeed emitted from traffic and industrial
 283 activities. Lower average amine concentrations on weekends were also observed during mobile
 284 measurements in Yangtze River Delta cities [Chang *et al.*, 2022].

285
 286

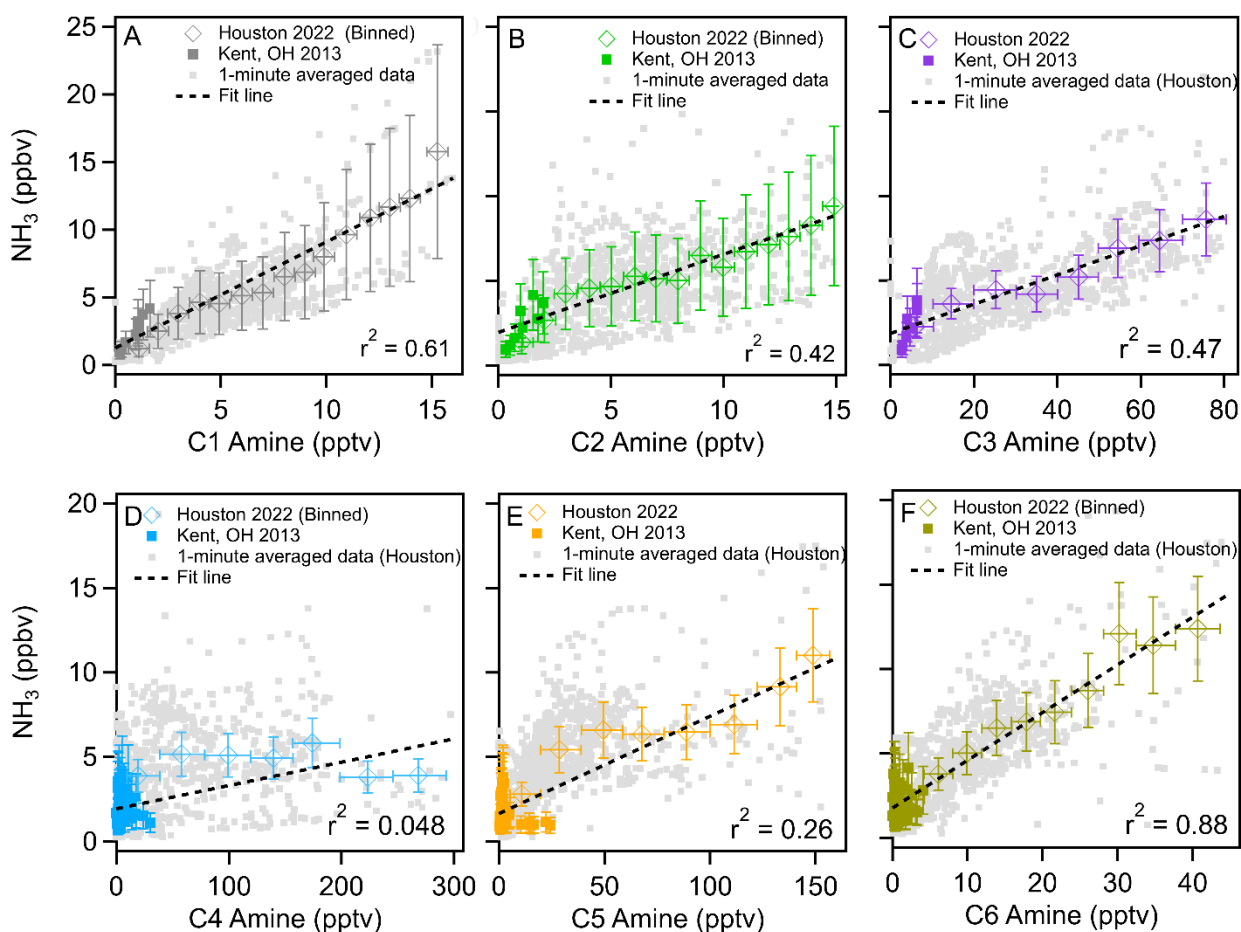


287
 288
 289 **Figure 6.** Wind rose plots of (a) ammonia and (b-g) C1-C6 amines observed in urban Houston.
 290 The color scale indicates concentration, and radial intensity shows wind speed.

291
 292 **4. Atmospheric Implications**

293
 294 Field observations show that sulfuric acid and amines are responsible for aerosol nucleation
 295 [J. Brean et al., 2020; R. Cai et al., 2021; Runlong Cai et al., 2023; Jen et al., 2016; Smith et al.,
 296 2010; Yan et al., 2021; Yao et al., 2016], however, currently, global models do not have amine
 297 emission inventories. Figure 7 shows the correlation of ammonia with C1-C6 amines measured
 298 during this campaign. This figure also includes that data obtained with the same instrument in
 299 Kent, Ohio, [You et al., 2014]. It is clear from this figure that concentrations of ammonia, C1, C2,
 300 C3, C5, and C6 amines were positively correlated with one another throughout the study: r^2 values
 301 for the correlation between ammonia and amines were 0.61 for C1, 0.42 for C2, 0.47 for C3, 0.26

302 for C5 and 0.88 for C6. These relationships imply that these compounds are mostly co-emitted
 303 from similar sources and undergo similar atmospheric transport. C4 amines showed no correlation
 304 with ammonia and lower-mass amines – the r^2 value for C4 vs. NH_3 was 0.048. This indicates a
 305 unique source for C4 amines, consistent with both elevated C4 concentrations at high wind speeds
 306 and higher weekend C4 concentrations as discussed previously. Correlations of C1-C3 amines
 307 concentrations, taken from the linear fits of the plots shown in Figure 7, were approximately
 308 equivalent to $1.1 \times 10^{-3} [\text{NH}_3]$, $1.4 \times 10^{-3} [\text{NH}_3]$, and $8.4 \times 10^{-3} [\text{NH}_3]$, respectively. C5 and C6
 309 amine concentrations were $1.9 \times 10^{-2} [\text{NH}_3]$ and $3.5 \times 10^{-3} [\text{NH}_3]$, respectively (Table S2). From
 310 these results, we propose that global modelers use 0.1 % of the ammonia concentration as a proxy
 311 of dimethylamine to simulate urban NPF processes. However, this recommendation comes with
 312 the caveat that measured C2 amines may include dimethylamine as well as ethylamine due to the
 313 inability of mass spectrometry to resolve isomers. Therefore, this correlation represents only the
 314 upper bound of dimethylamine concentrations.
 315



316
 317 **Figure 7.** Correlations of C1-C6 amines with ammonia throughout the observation period in
 318 Houston (diamonds) and Kent, OH (squares) as reported by [You et al., 2014]. Binned
 319 concentrations are shown in colored squares, 1-minute averaged data from Houston are shown in

320 gray squares. Vertical bars indicate one standard deviation from the mean values of observation
321 data. Horizontal bars indicate bin widths. Black dashed lines indicate linear fits of the combined
322 data from Kent and Houston.

323 **5. Conclusions**

324 Our observations in urban Houston show that ammonia and amines generally followed a clear
325 diurnal cycle, peaking in the early afternoon when the ambient temperature was highest during the
326 day. We found a correlation of ammonia and amines with ambient temperature. The pronounced
327 diurnal cycles and temperature dependence of these compounds may be due to active partitioning
328 between the gas and particle phases, which is sensitively dependent on temperature. This could be
329 due to increased emissions of ammonia and amines from biogenic and anthropogenic sources. It
330 is likely a combination of these effects that causes elevated ammonia and amine concentrations
331 when temperatures are high.

332 High concentrations of ammonia and amines were correlated with local air masses from
333 densely populated areas and areas of high traffic, industry, and other human activity. This suggests
334 that most ammonia and amines measured in Houston originated from pollutant sources, consistent
335 with the correlation observed with CO concentrations. There was also a clear increase in ammonia
336 and amines on days with more human activity as shown by the results of concentrations on
337 weekends vs weekdays. We observed a consistent relationship between ammonia and amines
338 during our measurement campaign as well as with observations in less densely populated Kent,
339 Ohio, suggesting that it is reasonable to parameterize amine emission inventories based on existing
340 ammonia inventories to simulate urban NPF processes. However, as the CIMS is incapable of
341 resolving amides or isomers, this parameterization is only capable of representing the upper
342 bounds of amines. Further work involving instrumentation capable of isomer resolution such as
343 tandem MS/MS or chromatographic separation is needed to determine typical isomer ratios of
344 amines for more accurate parameterizations.

345 The CIMS used in this campaign is currently one of the few instruments in the world that is
346 capable of simultaneous measurements of ammonia and amines at atmospherically relevant
347 detection limits and timescales. Studies have shown that the co-presence of ammonia and amines
348 can enhance sulfuric acid nucleation rates compared to ammonia alone [*Glusoe et al., 2015; Myllys*
349 *et al., 2019; Yu et al., 2012*]. From this perspective, simultaneous measurements of ammonia and
350 amines will be required for the correct prediction of NPF processes in the atmosphere.
351 Measurements of ammonia and amines with comprehensive calibration as shown in the present
352 study are very even rarer, but such measurements are needed for mitigating urban air quality
353 problems and the health effects of ultrafine particles.

354

355 **Author Contributions**

356 SHL designed the research; LT and SHL performed measurements; JF provided the measurement
357 platform as well as the trace gas and meteorology data; LT and SHL wrote the manuscript.

358 **Competing interests**

359 The authors declare that they have no conflict of interest.

360 **Acknowledgements**

361 We acknowledge funding support from National Science Foundation (grant numbers 2209722,
362 2117389, and 2107916) and Texas Commission on Environmental Quality (grant number 582-22-
363 31535-018).

364

365 **Table 1.** Ammonia and amine measurements with CIMS at various locations reported in the
 366 literature. DL, detection limit of each instrument.

Location	NH ₃ (ppbv)	C1 Amine (pptv)	C2 Amine (pptv)	C3 Amine (pptv)	C4 Amine (pptv)	C5 Amine (pptv)	C6 Amine (pptv)
Rural Alabama Forest [<i>You et al.</i> , 2014]*	Up to 1-2	< DL	< DL	1 - 10	< DL	< DL	< DL
Kent, Ohio [<i>You et al.</i> , 2014]*	Up to 6	1 – 4	< DL	5 - 10	10 - 50	10 - 100	< DL
Kent, Ohio [<i>Yu and Lee</i> , 2012]*	0.5 ± 0.26	-	8 ± 3	16 ± 7	-	-	-
Atlanta, Georgia [<i>Hanson et al.</i> , 2011]†	-	< 1	3	4 – 15	25	-	-
Lewes, Delaware [<i>Freshour et al.</i> , 2014]†	0.8	5	28	6	150	1	2
Lamont, Oklahoma [<i>Freshour et al.</i> , 2014]†	0.9	4	14	35	150	98	20
Minneapolis, Minnesota [<i>Freshour et al.</i> , 2014]†	1.8	4	42	19	14	20	5
Shanghai [<i>Yao et al.</i> , 2016]‡	-	3.9 ± 1.2	6.6 ± 1.2	0.4 ± 0.1	3.6 ± 1.0	0.7 ± 0.3	1.8 ± 0.8
Nanjing [<i>Zheng et al.</i> , 2015]‡	1.7 ± 2.3	7.2 ± 7.4 (C1 + C2 + C3)			-	-	-
Wangdu	-	-	14.6 ± 14.9	-	-	-	-

[Y Wang et al., 2020b]§							
Beijing [Zhu et al., 2022]‡	2.8 ± 2.0	5.2 ± 4.3 (C1 + C2 + C3)	-	-	-		
Houston, TX (This study)*	4 ± 1	4 ± 2	6 ± 2	31 ± 9	79 ± 30	33 ± 12	12 ± 4

367

368 * CIMS with ethanol reagent

369 † Proton-transfer chemical ionization mass spectrometer (PTR-CIMS)

370 ‡ High-resolution time of flight chemical ionization mass spectrometer (HR-TOF CIMS) with
 371 ethanol reagent

372 § Vocus proton transfer time-of-flight mass spectrometer (PTR-TOF MS)

373

374

375 **References**

- 376
- 377 Almeida, J., et al. (2013), Molecular understanding of sulphuric acid–amine particle nucleation
378 in the atmosphere, *Nature*, 502(7471), 359-363, doi:10.1038/nature12663.
- 379 Beck, L. J., et al. (2021), Differing Mechanisms of New Particle Formation at Two Arctic Sites,
380 *Geophysical Research Letters*, 48(4), e2020GL091334,
381 doi:<https://doi.org/10.1029/2020GL091334>.
- 382 Benson, D. R., A. Markovich, M. Al-Refai, and S. H. Lee (2010), A Chemical Ionization Mass
383 Spectrometer for ambient measurements of Ammonia, *Atmos. Meas. Tech.*, 3(4), 1075-1087,
384 doi:10.5194/amt-3-1075-2010.
- 385 Bianchi, F., et al. (2016), New particle formation in the free troposphere: A question of
386 chemistry and timing, *Science*, 352(6289), 1109-1112, doi:10.1126/science.aad5456.
- 387 Brean, J., D. C. S. Beddows, Z. Shi, B. Temime-Roussel, N. Marchand, X. Querol, A. Alastuey,
388 M. C. Minguillón, and R. M. Harrison (2020), Molecular insights into new particle formation in
389 Barcelona, Spain, *Atmos. Chem. Phys.*, 20(16), 10029-10045, doi:10.5194/acp-20-10029-2020.
- 390 Brean, J., M. Dall’Osto, R. Simó, Z. Shi, D. C. S. Beddows, and R. M. Harrison (2021), Open
391 ocean and coastal new particle formation from sulfuric acid and amines around the Antarctic
392 Peninsula, *Nature Geoscience*, 14(6), 383-388, doi:10.1038/s41561-021-00751-y.
- 393 Cai, R., et al. (2021), Sulfuric acid–amine nucleation in urban Beijing, *Atmos. Chem. Phys.*,
394 21(4), 2457-2468, doi:10.5194/acp-21-2457-2021.
- 395 Cai, R., et al. (2023), Significant contributions of trimethylamine to sulfuric acid nucleation in
396 polluted environments, *npj Climate and Atmospheric Science*, 6(1), 75, doi:10.1038/s41612-023-
397 00405-3.
- 398 Chang, Y., et al. (2022), Nonagricultural Emissions Dominate Urban Atmospheric Amines as
399 Revealed by Mobile Measurements, *Geophysical Research Letters*, 49(10), e2021GL097640,
400 doi:<https://doi.org/10.1029/2021GL097640>.
- 401 Ellis, R. A., J. G. Murphy, E. Pattey, R. van Haarlem, J. M. O'Brien, and S. C. Herndon (2010),
402 Characterizing a Quantum Cascade Tunable Infrared Laser Differential Absorption Spectrometer
403 (QC-TILDAS) for measurements of atmospheric ammonia, *Atmos. Meas. Tech.*, 3(2), 397-406,
404 doi:10.5194/amt-3-397-2010.
- 405 Erupe, M. E., et al. (2010), Correlation of aerosol nucleation rate with sulfuric acid and ammonia
406 in Kent, Ohio: An atmospheric observation, *Journal of Geophysical Research: Atmospheres*,
407 115(D23), doi:<https://doi.org/10.1029/2010JD013942>.
- 408 Erupe, M. E., A. A. Viggiano, and S. H. Lee (2011), The effect of trimethylamine on
409 atmospheric nucleation involving H₂SO₄, *Atmos. Chem. Phys.*, 11, 4767-4775.
- 410 Freshour, N. A., K. K. Carlson, Y. A. Melka, S. Hinz, B. Panta, and D. R. Hanson (2014), Amine
411 permeation sources characterized with acid neutralization and sensitivities of an amine mass
412 spectrometer, *Atmos. Meas. Tech.*, 7(10), 3611-3621, doi:10.5194/amt-7-3611-2014.
- 413 Ge, X., A. S. Wexler, and S. L. Clegg (2011a), Atmospheric amines – Part I. A review,
414 *Atmospheric Environment*, 45(3), 524-546, doi:<https://doi.org/10.1016/j.atmosenv.2010.10.012>.
- 415 Ge, X., A. S. Wexler, and S. L. Clegg (2011b), Atmospheric amines – Part II. Thermodynamic
416 properties and gas/particle partitioning, *Atmospheric Environment*, 45(3), 561-577,
417 doi:<https://doi.org/10.1016/j.atmosenv.2010.10.013>.
- 418 Glasoe, W. A., K. Volz, B. Panta, N. Freshour, R. Bachman, D. R. Hanson, P. H. McMurry, and
419 C. Jen (2015), Sulfuric acid nucleation: an experimental study of the effect of seven bases, *J.*
420 *Geophys. Res.*, 120, 1933-1950, doi:Doi: 10.1002/2014JD022730.

421 Griffith, D. W. T., and B. Galle (2000), Flux measurements of NH₃, N₂O and CO₂ using dual
422 beam FTIR spectroscopy and the flux–gradient technique, *Atmospheric Environment*, 34(7),
423 1087-1098, doi:[https://doi.org/10.1016/S1352-2310\(99\)00368-4](https://doi.org/10.1016/S1352-2310(99)00368-4).

424 Gu, B., et al. (2021), Abating ammonia is more cost-effective than nitrogen oxides for mitigating
425 PM_{2.5} air pollution, *Science*, 374(6568), 758-762, doi:10.1126/science.abf8623.

426 Hanson, D. R., P. H. McMurry, J. Jiang, D. Tanner, and L. G. Huey (2011), Ambient Pressure
427 Proton Transfer Mass Spectrometry: Detection of Amines and Ammonia, *Environmental Science
428 & Technology*, 45(20), 8881-8888, doi:10.1021/es201819a.

429 Jen, C. N., R. Bachman, J. Zhao, P. H. McMurry, and D. R. Hanson (2016), Diamine-sulfuric
430 acid reactions are a potent source of new particle formation, *Geophysical Research Letters*,
431 43(2), 867-873, doi:<https://doi.org/10.1002/2015GL066958>.

432 Jokinen, T., et al. Ion-induced sulfuric acid–ammonia nucleation drives particle formation in
433 coastal Antarctica, *Science Advances*, 4(11), eaat9744, doi:10.1126/sciadv.aat9744.

434 Köllner, F., et al. (2017), Particulate trimethylamine in the summertime Canadian high Arctic
435 lower troposphere, *Atmos. Chem. Phys.*, 17(22), 13747-13766, doi:10.5194/acp-17-13747-2017.

436 Kürten, A., A. Bergen, M. Heinritzi, M. Leiminger, V. Lorenz, F. Piel, M. Simon, R. Sitals, A.
437 C. Wagner, and J. Curtius (2016), Observation of new particle formation and measurement of
438 sulfuric acid, ammonia, amines and highly oxidized organic molecules at a rural site in central
439 Germany, *Atmos. Chem. Phys.*, 16(19), 12793-12813, doi:10.5194/acp-16-12793-2016.

440 Lee, S.-H. (2022), Perspective on the Recent Measurements of Reduced Nitrogen Compounds in
441 the Atmosphere, *Frontiers in Environmental Science*, 10, doi:10.3389/fenvs.2022.868534.

442 Leen, J. B., X.-Y. Yu, M. Gupta, D. S. Baer, J. M. Hubbe, C. D. Kluzek, J. M. Tomlinson, and
443 M. R. Hubbell, II (2013), Fast In Situ Airborne Measurement of Ammonia Using a Mid-Infrared
444 Off-Axis ICOS Spectrometer, *Environmental Science & Technology*, 47(18), 10446-10453,
445 doi:10.1021/es401134u.

446 Lehtipalo, K., et al. (2018), Multicomponent new particle formation from sulfuric acid,
447 ammonia, and biogenic vapors, *Science Advances*, 4(12), eaau5363, doi:10.1126/sciadv.aau5363.

448 Liu, R., et al. (2024), Characteristics and sources of atmospheric ammonia at the SORPES
449 station in the western Yangtze river delta of China, *Atmospheric Environment*, 318, 120234,
450 doi:<https://doi.org/10.1016/j.atmosenv.2023.120234>.

451 Malloy, Q. G. J., Q. Li, B. Warren, D. R. Cocker III, M. E. Erupe, and P. J. Silva (2009),
452 Secondary organic aerosol formation from primary aliphatic amines with NO₃
453 radical, *Atmos. Chem. Phys.*, 9(6), 2051-2060, doi:10.5194/acp-9-2051-2009.

454 Martin, N. A., V. Ferracci, N. Cassidy, and J. A. Hoffnagle (2016), The application of a cavity
455 ring-down spectrometer to measurements of ambient ammonia using traceable primary standard
456 gas mixtures, *Applied Physics B*, 122(8), 219, doi:10.1007/s00340-016-6486-9.

457 McManus, J. B., S. Z. Mark, D. N. David, Jr., H. S. Joanne, C. H. Scott, C. W. Ezra, and W.
458 Rick (2010), Application of quantum cascade lasers to high-precision atmospheric trace gas
459 measurements, *Optical Engineering*, 49(11), 111124, doi:10.1117/1.3498782.

460 Miller, D. J., K. Sun, L. Tao, M. A. Khan, and M. A. Zondlo (2014), Open-path, quantum
461 cascade-laser-based sensor for high-resolution atmospheric ammonia measurements, *Atmos.
462 Meas. Tech.*, 7(1), 81-93, doi:10.5194/amt-7-81-2014.

463 Myllys, N., S. Chee, T. Olenius, M. Lawler, and J. Smith (2019), Molecular-Level
464 Understanding of Synergistic Effects in Sulfuric Acid–Amine–Ammonia Mixed Clusters, *The
465 Journal of Physical Chemistry A*, 123(12), 2420-2425, doi:10.1021/acs.jpca.9b00909.

466 Nielsen, C. J. (2016), Atmospheric Degradation of Amines (ADA). Summary report: Photo-
467 oxidation of methylamine, dimethylamine and trimethylamine. CLIMIT project no. 201604.,
468 *Norge: Norsk Institutt for Luftforskning*.

469 Nielsen, C. J., H. Herrmann, and C. Weller (2012), Atmospheric chemistry and environmental
470 impact of the use of amines in carbon capture and storage (CCS), *Chemical Society Reviews*,
471 *41*(19), 6684-6704, doi:10.1039/C2CS35059A.

472 Nowak, J. B., et al. (2006), Analysis of urban gas phase ammonia measurements from the 2002
473 Atlanta Aerosol Nucleation and Real-Time Characterization Experiment (ANARChE), *Journal*
474 *of Geophysical Research: Atmospheres*, *111*(D17), doi:<https://doi.org/10.1029/2006JD007113>.

475 Nowak, J. B., J. A. Neuman, R. Bahreini, C. A. Brock, A. M. Middlebrook, A. G. Wollny, J. S.
476 Holloway, J. Peischl, T. B. Ryerson, and F. C. Fehsenfeld (2010), Airborne observations of
477 ammonia and ammonium nitrate formation over Houston, Texas, *Journal of Geophysical*
478 *Research: Atmospheres*, *115*(D22), doi:<https://doi.org/10.1029/2010JD014195>.

479 Petrus, M., C. Popa, and A. M. Bratu (2022), Ammonia Concentration in Ambient Air in a Peri-
480 Urban Area Using a Laser Photoacoustic Spectroscopy Detector, *Materials (Basel)*, *15*(9),
481 doi:10.3390/ma15093182.

482 Pollack, I. B., J. Lindaas, J. R. Roscioli, M. Agnese, W. Permar, L. Hu, and E. V. Fischer (2019),
483 Evaluation of ambient ammonia measurements from a research aircraft using a closed-path QC-
484 TILDAS operated with active continuous passivation, *Atmos. Meas. Tech.*, *12*(7), 3717-3742,
485 doi:10.5194/amt-12-3717-2019.

486 Pushkarsky, M. B., M. E. Webber, O. Baghdassarian, L. R. Narasimhan, and C. K. N. Patel
487 (2002), Laser-based photoacoustic ammonia sensors for industrial applications, *Applied Physics*
488 *B*, *75*(2), 391-396, doi:10.1007/s00340-002-0967-8.

489 Qiu, C., and R. Zhang (2013), Multiphase chemistry of atmospheric amines, *Physical Chemistry*
490 *Chemical Physics*, *15*(16), 5738-5752, doi:10.1039/C3CP43446J.

491 Schwab, J. J., Y. Li, M. S. Bae, K. L. Demerjian, J. Hou, X. Zhou, B. Jensen, and S. C. Pryor
492 (2007), A laboratory intercomparison of real-time gaseous ammonia measurement methods,
493 *Environ Sci Technol*, *41*(24), 8412-8419, doi:10.1021/es070354r.

494 Silva, P. J., M. E. Erupe, D. Price, J. Elias, Q. G. J. Malloy, Q. Li, B. Warren, and D. R. Cocker,
495 III (2008), Trimethylamine as Precursor to Secondary Organic Aerosol Formation via Nitrate
496 Radical Reaction in the Atmosphere, *Environmental Science & Technology*, *42*(13), 4689-4696,
497 doi:10.1021/es703016v.

498 Smith, J. N., K. C. Barsanti, H. R. Friedli, M. Ehn, M. Kulmala, D. R. Collins, J. H. Scheckman,
499 B. J. Williams, and P. H. McMurry (2010), Observations of aminium salts in atmospheric
500 nanoparticles and possible climatic implications, *Proc. Natl. Acad. Sci.*, *107*(15), 6634-6639.

501 Wang, G., et al. (2016), Persistent sulfate formation from London Fog to Chinese haze,
502 *Proceedings of the National Academy of Sciences*, *113*(48), 13630-13635,
503 doi:10.1073/pnas.1616540113.

504 Wang, M., et al. (2020a), Rapid growth of new atmospheric particles by nitric acid and ammonia
505 condensation, *Nature*, *581*(7807), 184-189, doi:10.1038/s41586-020-2270-4.

506 Wang, Y., G. Yang, Y. Lu, Y. Liu, J. Chen, and L. Wang (2020b), Detection of gaseous
507 dimethylamine using vocus proton-transfer-reaction time-of-flight mass spectrometry,
508 *Atmospheric Environment*, *243*, 117875, doi:<https://doi.org/10.1016/j.atmosenv.2020.117875>.

509 Xiao, M., et al. (2021), The driving factors of new particle formation and growth in the polluted
510 boundary layer, *Atmos. Chem. Phys.*, *21*(18), 14275-14291, doi:10.5194/acp-21-14275-2021.

511 Xiao, S., et al. (2015), Strong atmospheric new particle formation in winter in urban Shanghai,
512 China, *Atmos. Chem. Phys.*, *15*(4), 1769-1781, doi:10.5194/acp-15-1769-2015.

513 Yan, C., et al. (2021), The Synergistic Role of Sulfuric Acid, Bases, and Oxidized Organics
514 Governing New-Particle Formation in Beijing, *Geophysical Research Letters*, *48*(7),
515 e2020GL091944, doi:<https://doi.org/10.1029/2020GL091944>.

516 Yao, L., et al. (2016), Detection of atmospheric gaseous amines and amides by a high-resolution
517 time-of-flight chemical ionization mass spectrometer with protonated ethanol reagent ions,
518 *Atmos. Chem. Phys.*, *16*(22), 14527-14543, doi:10.5194/acp-16-14527-2016.

519 You, Y., et al. (2014), Atmospheric amines and ammonia measured with a Chemical Ionization
520 Mass Spectrometer (CIMS), *Atmos. Chem. Phys.*, *14*, 12181-12194, doi:Doi: 10.5194/acpd-14-
521 16411-2014.

522 Yu, H., and S. H. Lee (2012), A chemical ionization mass spectrometer for the detection of
523 atmospheric amines, *Environ. Chem.*, *9*, 190-201.

524 Yu, H., R. McGraw, and S. H. Lee (2012), Effects of amines on formation of sub-3 nm particles
525 and their subsequent growth, *Geophys. Res. Lett.*, *39*, Doi: 10.1029/2011gl050099,
526 doi:10.1029/2011gl050099.

527 Zheng, J., Y. Ma, M. Chen, Q. Zhang, L. Wang, A. F. Khalizov, L. Yao, Z. Wang, X. Wang, and
528 L. Chen (2015), Measurement of atmospheric amines and ammonia using the high resolution
529 time-of-flight chemical ionization mass spectrometry, *Atmospheric Environment*, *102*, 249-259,
530 doi:<https://doi.org/10.1016/j.atmosenv.2014.12.002>.

531 Zhu, S., et al. (2022), Observation and Source Apportionment of Atmospheric Alkaline Gases in
532 Urban Beijing, *Environmental Science & Technology*, *56*(24), 17545-17555,
533 doi:10.1021/acs.est.2c03584.

534